RCM

Characterization of a [(O$_{3/2}$SiMe)$_x$(OSi(OH)Me)$_y$(OSiMe$_2$)$_z$] silsesquioxane copolymer resin by mass spectrometry

Ron E. Tecklenburg[1], William E. Wallace[2]* and Huiping Chen[1]

[1]Dow Corning Corporation, Analytical Sciences Department, Midland, MI 48686-0994
[2]National Institute of Standards and Technology, Polymers Division, Gaithersburg, MD 20899-8541

Electrospray ionization Fourier transform ion cyclotron resonance (ESI-FTICR) mass spectrometry and matrix-assisted laser desorption/ionization time-of-flight (MALDI-TOF) mass spectrometry were applied to a complex silsesquioxane-siloxane copolymer resin. The wide-polydispersity starting material was fractionated into 21 separate fractions in order to facilitate the analysis by mass spectrometry. ESI-FTICR exact mass measurements were able to identify the specific oligomers present in the lowest mass fractions and showed that very few unreacted silanol groups remained, that is, topologically closed structures predominated. MALDI-TOFMS was able to show that gel-permeation chromatography substantially underestimated the molecular masses of the higher mass fractions. Mass autocorrelation was able to show that the silsesquioxane monomer appeared only in even numbers in any given oligomer. This is a natural consequence of the highly condensed nature of the resin. Copyright © 2001 John Wiley & Sons, Ltd.

Silsesquioxanes, also termed three-dimensional organosilicon resins, have a long history in the materials science community and continue to generate much interest due to their unique structures and physical properties.[1–4] One particular structure type, methyl silsesquioxane nanotubes, is similar to carbon-based fullerenes and nanotubes except that the silsesquioxane-based resins form at room temperature by simple acid-catalyzed hydrolysis and condensation chemistries. The application areas for silicone resins range from (i) protective coatings to insulate from heat, abrasion, or electricity, (ii) processing aids or modifiers for organic polymers, (iii) low-k interlayer dielectrics for microelectronics, and (iv) precursors to crystalline silicon carbide ceramics. While silsesquioxane resins have been commercially highly successful, very little detailed information exists about their molecular structure due to the extremely complex nature of the individual molecules present in the resin. Literally hundreds of individual structures exist in typical silsesquioxane resins and many of these species cannot be identified without the use of high-resolution mass spectrometry techniques.[4–6] The (O$_{3/2}$SiMe)$_x$(OSi(OH)Me)$_y$(OSiMe$_2$)$_z$ silsesquioxane resin studied here was synthesized by reaction of MeSiCl$_3$ and Me$_2$SiCl$_2$ at an 85:15 molar ratio in a water/isopropanol/toluene solvent system. Initially, the MeSiCl$_3$ and Me$_2$SiCl$_2$ silanes react with water to produce methylhydroxysilane intermediates and HCl. The silanol groups present on the methylhydroxysilanes can then undergo further reaction *via* intermolecular and intramolecular condensation reactions to produce a complex distribution of monomethyl/dimethylsilsesquioxane species. Once the reaction is complete, the HCl and isopropanol are removed by rinsing with water. Finally, the toluene solution is stripped until 50% solids remain dissolved. This final resin product was subsequently fraction-ated by supercritical fluid extraction into 21 distinct fractions with narrower polydispersities, thereby making them much more amenable to mass spectrometric analysis than the initial resin.[7] Extensive characterization by mass spectrometry of the fractions of this complex silsesquioxane resin is reported here.

EXPERIMENTAL

ESI-FTICR

All experiments were performed using a Bruker (Billerica, MA, USA) Apex II Fourier transform ion cyclotron resonance (FTICR) mass spectrometer equipped with a 4.7 T superconducting magnet and an external Analytica electrospray ionization (ESI) source (Branford, CT, USA). A Cole-Parmer (Vernon Hills, IL, USA) series 74900 syringe pump was used to continuously infuse samples into the ESI source at a flow rate of 0.3 mL h^{-1}. The external electrospray ion source was operated with a 45° off-axis sprayer. High purity (99.995%) nitrogen gas was used as both nebulizing gas at ambient temperature and as a drying gas at 105°C. An electrostatic potential of *ca.* −4.7 kV (relative to the grounded needle) was applied to the metal-capped glass capillary. Ions were accumulated in a hexapole ion guide, adjacent to the external ESI source, and were subsequently injected into the INFINITY™ cell using the patented Sidekick™ method. Data

Correspondence to: W. E. Wallace, National Institute of Standards and Technology, Polymers Division, 100 Bureau Drive Stop 8541, Gaithersburg, MD 20899-8541, USA.
E-mail: william.wallace@nist.gov
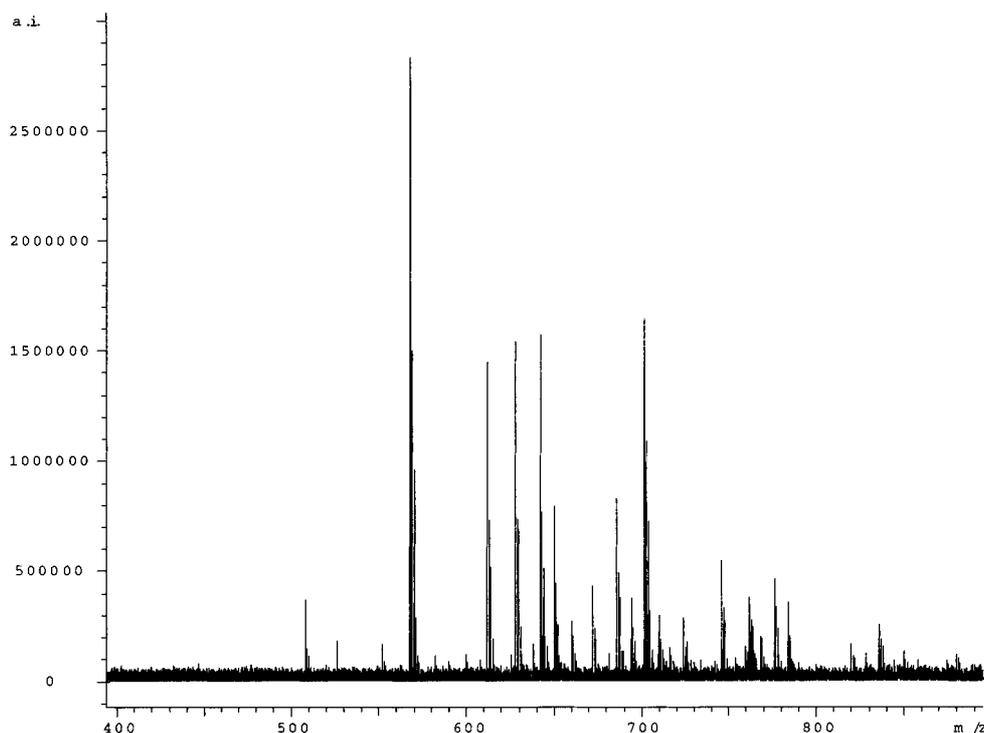
Figure 1. ESI-FTICR mass spectrum of fraction 1.

acquired in the broadband mode and heterodyne mode were typically collected using 512 k data points and 32 k data points, respectively. The instrument was calibrated with a Dow Corning standard consisting of cyclic polydimethyl-siloxane (PDMS) structures (OSiMe2)$_x$; where x = 3,6,9 …42 spanning a molecular mass range of 222 u through 3108 u.

All resin samples and cyclic poly(dimethyl siloxane) standards were obtained within the Dow Corning Research Center in Midland, Michigan. The sample and standards were prepared for ESI analysis by dissolving *ca.* 20 nL into 5 mL of a 1:1 mixture of $CHCl_3$/MeOH. 1 mM of ammonium acetate salt (Fisher Scientific) was intentionally added to the MeOH phase to assist the ionization of silicone materials. In general silicones are relatively non-polar and cannot be readily ionized by electrospray mass spectrometry without the addition of ammonium salts (or alkali metal salts) to assist in the ionization process. In the positive-ion mode using ammonium acetate, typically only $[M + NH_4]^+$ ions are detected in the ESI-FTICRMS experiment with little or no fragmentation.

MALDI-TOFMS

The data were taken on a Bruker Reflex II time-of-flight mass spectrometer using delayed ion extraction and reflectron ion optics to improve mass resolution. The analyte fractions were dissolved in acetone, as was the 3,5-dimethoxy-4-hydroxycinnamic acid matrix (Aldrich). The matrix acts as a carrier to assist with the ionization of the analyte upon pulsed irradiation with a 337 nm nitrogen laser. The nominal mass ratio of matrix to analyte was 13:1. The analyte + matrix mixture in acetone was electrosprayed at 5 kV in ambient onto a stainless steel target (during which the solvent evaporates).[8] The solid mixture of analyte + matrix

was then laser ablated in vacuum to create intact oligomer ions with adventitious sodium (Na^+) cationization. Laser power was kept just above desorption threshold. Electro-static deflection was used to keep the intense matrix signal (appearing at short flight times) from saturating the microchannel plate detectors. Each spectrum represents the sum of 250 discrete laser shots each having about 2 µJ of energy over a spot size of 250 µm by 50 µm.

GPC

The gel-permeation chromatography (GPC) was performed using Polymer Laboratories mixed E and mixed D columns at 35 °C using a refractive index detector. The flow rate was 1.0 mL/min with an injection volume of 100 µL. The injected solution had a mass fraction of 0.5% to 1.0% polymer in degassed THF. Polystyrene standards were used for calibration.

RESULTS

Individual fractions from the super critical fluid extraction (SFE) of the bulk methyl silsesquioxane resin were characterized by mass spectrometry. Specifically, fractions 1 and 4 were analyzed by ESI-FTICR while fractions 4, 8 13, 18, 20, 21 were analyzed by MALDI-TOFMS.

ESI-FTICR

Fraction 1, shown in Fig. 1, contains the lowest molecular mass components while fraction 4, shown in Fig. 2, contains higher molecular mass components and a very large number of individual molecules that comprise the sample. The mass spectrum acquired for fraction 1 consists of ions whose molecular masses span 500 u to 800 u, while the mass
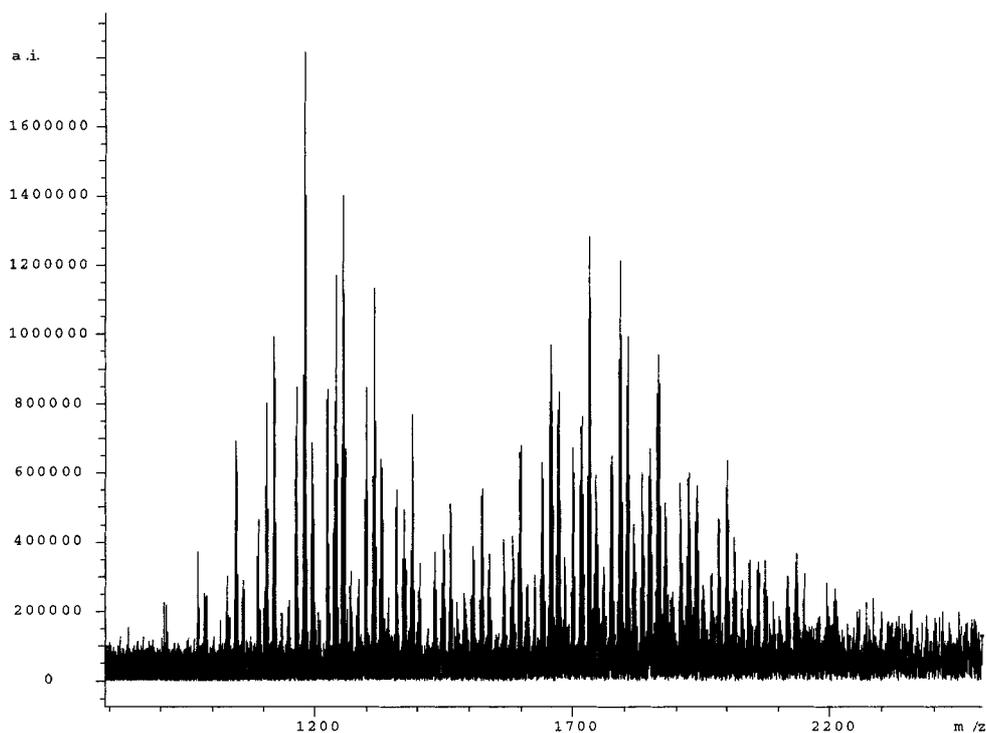
Figure 2. ESI-FTICR mass spectrum of fraction 4.

spectrum collected for fraction 4 contains ions with molecular masses between 900 u and 2200 u. The resultant FTICR mass spectra were acquired in the broadband mode, typically resulting in mass resolving powers, $m/\Delta m$, of 30 000 to 50 000. This mass spectral resolution was found to be sufficient to adequately separate isobaric ions present in the mixture of species comprising the SFE fractionated silsesquioxane resin samples. For example, Fig. 3 contains an expanded view of the 686 u to 690 u region of the FTICR mass spectrum of silsesquioxane resin fraction 1. While the ions at 686.07155 u, 687.06816 u and 688.06909 u represent the ^{28}Si, ^{29}Si and ^{30}Si isotopes of the structure
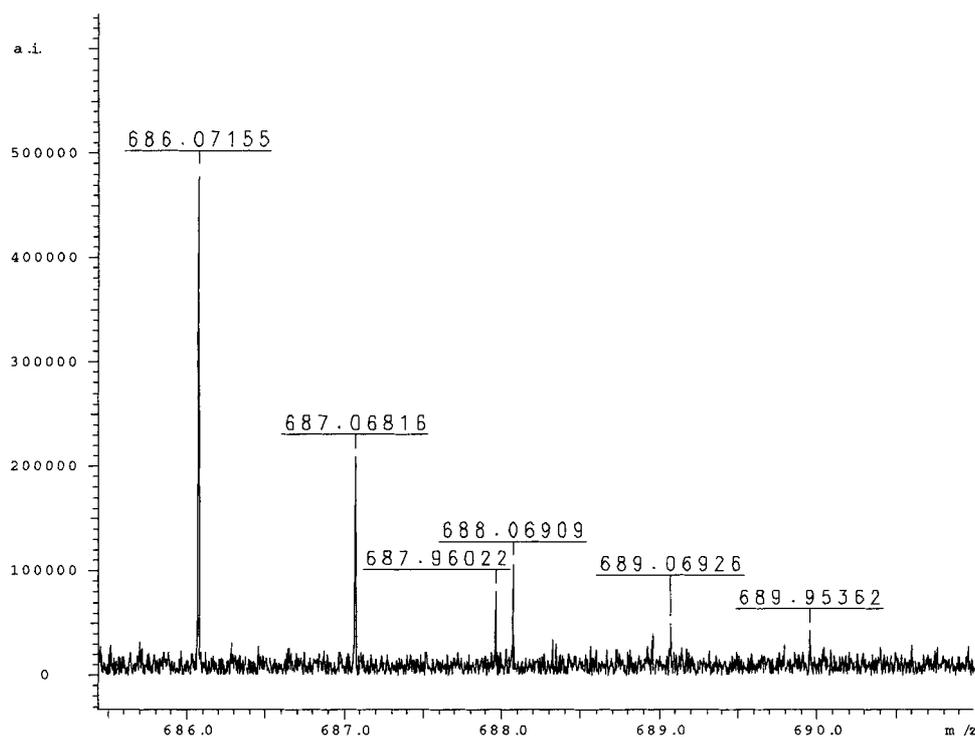
Figure 3. Expanded view of the ESI-FTICR mass spectrum of fraction 1.

Table 1. Methyl silsesquioxane structural assignments from the high resolution ESI-FTICR data for fraction 1

Silsesquioxane structure	Structure letter	Measured mass $[M + NH_4]^+$	Theoretical mass $[M + NH_4]^+$	Mass error (ppm)
$[O_{3/2}SiMe]_4[OSiMe_2]_3$	**A**	508.05926	508.06168	−4.8
$[O_{3/2}SiMe]_4[OSiMe_2]_2[OSi(OiPr)Me]$	**B**	552.08847	552.08792	1.0
$[O_{3/2}SiMe]_6[OSiMe_2]_2$	**C**	568.02737	568.02841	−1.8
$[O_{3/2}SiMe]_6[OSiMe_2][OSi(OH)Me]$	**D**	570.0073	570.00773	−0.8
$[O_{3/2}SiMe]_4[OSiMe_2]_2[OSi(OH)Me][OSi(OMe)Me]$	**E**	600.05153	600.05426	−4.5
$[O_{3/2}SiMe]_6[OSiMe_2][OSi(OiPr)Me]$	**D**	612.05018	612.05465	−7.3
$[O_{3/2}SiMe]_8[OSiMe_2]$	**F**	627.99404	627.99514	−1.8
$[O_{3/2}SiMe]_6[OSiMe_2]_3$	**G**	642.04653	642.04718	−1.0
$[O_{3/2}SiMe]_6[OSiMe_2]_2[OSi(OH)Me]$	**H**	644.02597	644.0265	−0.8
$[O_{3/2}SiMe]_6[OSiMe_2][OSi(OH)Me][OSi(OMe)Me]$	**I**	660.01766	660.02144	−5.7
$[O_{3/2}SiMe]_8[OSi(OiPr)Me]$	**J**	672.01602	672.02102	−7.4
$[O_{3/2}SiMe]_6[OSiMe_2]_2[OSi(OiPr)Me]$	**H**	686.07155	686.07342	−2.7
$[O_{3/2}SiMe]_{10}$	**K**	687.96022	687.96187	−2.4
$[O_{3/2}SiMe]_8[OSiMe_2]_2$	**L**	702.01118	702.01391	−3.9
$[O_{3/2}SiMe]_8[OSiMe_2][OSi(OH)Me]$	**M**	703.99192	703.99323	−1.9
$[O_{3/2}SiMe]_8[OSiMe_2][OSi(OiPr)Me]$	**M**	746.03767	746.04015	−3.3
$[O_{3/2}SiMe]_{10}[OSiMe_2]$	**N**	761.97722	761.98064	−4.5
$[O_{3/2}SiMe]_8[OSiMe_2]_3$	**O**	776.03379	776.03268	1.4

$[O_{3/2}SiMe]_6[OSiMe_2]_2[OSi(OiPr)Me]$, the ion at 687.96022 u (corresponding to the $[O_{3/2}SiMe]_{10}$ structure) is easily resolved from the 688.06909 u ion approximately 0.1 u apart. Typically, mass accuracies of less than 5 ppm were achieved from the ESI-FTICR exact mass data, thereby leading to the unambiguous assignment of empirical molecular formulae. Tables 1 and 2 list the theoretical and empirically measured exact masses, and their mass errors, for the major ions observed in the mass spectra of fractions 1 and 4, respectively. In addition, the methyl silsesquioxane resin structural assignments for fractions 1 and 4 are also listed in these tables. These structural assignments were obtained by comparing the empirically measured exact masses with the exact masses of plausible structures containing various numbers of the five known siloxy groups present in the system, $[O_{3/2}SiMe]$, $[OSiMe_2]$, $[OSi(OH)Me]$, $[OSi(OMe)Me]$ and $[OSi(OiPr)Me]$. More specifically, a Fortran 90 computer algorithm[9] (developed at Dow Corning) was used for the purpose of identifying possible silsesquioxane structures for each of the molecular ions observed in the FTICR electrospray spectra. As inputs to the program, one simply identifies the measured exact masses, the siloxy groups present in the system as well as the range of numbers for each siloxy group. The output lists all possible silsesquioxane structures whose masses are within ±0.2 u of the measured exact mass. For each of the structural assignments made in Tables 1 and 2, only one siloxane structure could be found to fit the experimentally measured exact mass to within 10 ppm for each unknown. Thus, no ambiguous structural assignments exist for the data presented in Tables 1 and 2.

For the detected and identified silsesquioxane species listed in Table 1, a corresponding letter (**A** through **O**) has been assigned to each structure within the table. These structures consist of incompletely closed (condensed) siloxane cages whose faces are predominately made up of rings containing four and five silicon (and alternating oxygen) atoms. For illustrative purposes, three-dimensional draw-

ings for each structure in Table 1 are presented in Fig. 4. No such attempt was made to draw three-dimensional structures for the resin species identified in Table 2, due to the complexity of the images, and the very large number of possible isomers present. Each chemical drawing in Fig. 4 contains an even number of methyl siloxy groups $[O_{3/2}SiMe]$ and can also contain one or more of the four following groups: $[OSiMe_2]$, $[OSi(OH)Me]$, $[OSi(OMe)Me]$, or $[OSi(OiPr)Me]$. These five siloxane environments are abbreviated as T, D, $T^{(OH)}$, $T^{(OMe)}$ and $T^{(OiPr)}$, respectively. Below each of the three-dimensional structures drawn in Fig. 4, only the abbreviated shorthand representation of the structure is used. For example, the first identified structure (**A**) in Table 1, $[O_{3/2}SiMe]_4[OSiMe_2]_3$, is abbreviated as T_4D_3 in Fig. 4. Many of the identified silsesquioxane structures in Table 1 can exist as multiple isomers. Only one or two isomers for each siloxane cage structure are drawn in Fig. 4. As examples, structures **A** (T_4D_3) and **C** (T_6D_2) are each drawn as two discrete isomers. For structures **A** through **O**, many isomeric forms may exist in the silsesquioxane resin as it is synthesized. The predominance of one isomer over the others will only occur in cases where the partially condensed three-dimensional orientation of the hydroxyl and methyl groups on neighboring silicon atoms is fixed as the condensation steps proceed. This can occur when the resin synthesis is performed in a two-phase solvent system; hydrophobic organic solvent containing the initial chlorosilane and a hydrophilic aqueous phase. As the chlorosilane is hydrolyzed to hydroxysilanes, the hydroxysilanes will migrate into the water phase with relatively fixed orientations, thus producing linear and cyclic precursor siloxanes with predominately *cis*-orientations of the silanol groups. It should be noted, however, that the presence of HCl produced during the synthesis of the resin (from $MeSiCl_3$ and Me_2SiCl_2 hydrolysis) will likely cause siloxane bond cleavages and rearrangements. Thus, the resin product is expected to be composed of a variety of three-dimensional isomeric structures for each resin species that is produced.

RCM

Table 2. Methyl silsesquioxane structural assignments from the high resolution ESI-FTICR data for fraction 4

Silsesquioxane structure	Measured mass $[M + NH_4]^+$	Theoretical mass $[M + NH_4]^+$	Mass error (ppm)
$[O_{3/2}SiMe]_{12}[OSiMe_2]_2$	969.98005	969.98491	−5.0
$[O_{3/2}SiMe]_{10}[OSiMe_2]_4$	984.03681	984.03695	−0.1
$[O_{3/2}SiMe]_{10}[OSiMe_2]_3[OSi(OH)Me]$	986.01048	986.01599	−5.6
$[O_{3/2}SiMe]_{10}[OSiMe_2]_2[OSi(OH)Me][OSi(OMe)Me]$	1002.00836	1002.01091	−2.5
$[O_{3/2}SiMe]_{12}[OSiMe_2][OSi(OiPr)Me]$	1014.00768	1014.01091	−3.2
$[O_{3/2}SiMe]_{10}[OSiMe_2]_3[OSi(OiPr)Me]$	1028.05949	1028.06319	−3.6
$[O_{3/2}SiMe]_{12}[OSiMe_2]_3$	1043.99970	1044.00368	−3.8
$[O_{3/2}SiMe]_{12}[OSiMe_2]_2[OSi(OH)Me]$	1045.97985	1045.98275	−2.8
$[O_{3/2}SiMe]_{10}[OSiMe_2]_5$	1058.05688	1058.0572	1.1
$[O_{3/2}SiMe]_{12}[OSiMe_2]_2[OSi(OiPr)Me]$	1088.02718	1088.02992	−2.5
$[O_{3/2}SiMe]_{10}[OSiMe_2]_4[OSi(OiPr)Me]$	1102.07515	1102.08196	−6.2
$[O_{3/2}SiMe]_{14}[OSiMe_2]_2$	1103.96853	1103.97041	−1.7
$[O_{3/2}SiMe]_{12}[OSiMe_2]_4$	1118.02215	1118.02245	−0.3
$[O_{3/2}SiMe]_{12}[OSiMe_2]_3[OSi(OH)Me]$	1119.99578	1120.00154	−5.1
$[O_{3/2}SiMe]_{10}[OSiMe_2]_5[OSi(OH)Me]$	1134.05051	1134.05381	−2.9
$[O_{3/2}SiMe]_{14}[OSiMe_2][OSi(OiPr)Me]$	1147.99840	1147.99645	1.7
$[O_{3/2}SiMe]_{12}[OSiMe_2]_3[OSi(OiPr)Me]$	1162.04960	1162.04869	0.8
$[O_{3/2}SiMe]_{16}[OSiMe_2]$	1163.93796	1163.93714	0.7
$[O_{3/2}SiMe]_{14}[OSiMe_2]_3$	1177.98759	1177.98918	−1.3
$[O_{3/2}SiMe]_{12}[OSiMe_2]_5$	1192.04421	1192.04107	2.6
$[O_{3/2}SiMe]_{12}[OSiMe_2]_3[OSi(OH)Me][OSi(OMe)Me]$	1210.01882	1210.01524	3.0
$[O_{3/2}SiMe]_{14}[OSiMe_2]_2[OSi(OiPr)Me]$	1222.01463	1222.01542	−0.6
$[O_{3/2}SiMe]_{12}[OSiMe_2]_4[OSi(OiPr)Me]$	1236.07174	1236.06746	3.5
$[O_{3/2}SiMe]_{16}[OSiMe_2]_2$	1237.95839	1237.95591	2.0
$[O_{3/2}SiMe]_{14}[OSiMe_2]_4$	1252.00713	1252.00795	−0.7
$[O_{3/2}SiMe]_{14}[OSiMe_2][OSi(OiPr)Me]_2$	1266.05259	1266.04166	8.6
$[O_{3/2}SiMe]_{12}[OSiMe_2]_3[OSi(OiPr)Me]_2$	1280.10006	1280.09370	5.0
$[O_{3/2}SiMe]_{16}[OSiMe_2][OSi(OiPr)Me]$	1281.98171	1281.98200	−0.2
$[O_{3/2}SiMe]_{14}[OSiMe_2]_3[OSi(OiPr)Me]$	1296.03419	1296.03419	0.0
$[O_{3/2}SiMe]_{12}[OSiMe_2]_5[OSi(OiPr)Me]$	1310.09049	1310.08607	3.4
$[O_{3/2}SiMe]_{16}[OSiMe_2]_3$	1312.97610	1311.97468	1.1
$[O_{3/2}SiMe]_{14}[OSiMe_2]_5$	1326.02459	1326.02672	−1.6
$[O_{3/2}SiMe]_{14}[OSiMe_2]_4[OSi(OH)Me]$	1328.00649	1328.00588	0.5
$[O_{3/2}SiMe]_{14}[OSiMe_2]_2[OSi(OiPr)Me]_2$	1340.05316	1340.06043	−5.4
$[O_{3/2}SiMe]_{16}[OSiMe_2]_2[OSi(OiPr)Me]$	1355.99812	1356.00079	−2.0
$[O_{3/2}SiMe]_{14}[OSiMe_2]_4[OSi(OiPr)Me]$	1370.05822	1370.05296	3.8
$[O_{3/2}SiMe]_{18}[OSiMe_2]_2$	1371.93276	1371.94141	−6.3
$[O_{3/2}SiMe]_{16}[OSiMe_2]_4$	1385.99476	1385.99345	0.9
$[O_{3/2}SiMe]_{16}[OSiMe_2][OSi(OiPr)Me]_2$	1400.02100	1400.02716	−4.4
$[O_{3/2}SiMe]_{16}[OSiMe_2]_3[OSi(OiPr)Me]$	1430.01900	1430.01969	−0.5
$[O_{3/2}SiMe]_{14}[OSiMe_2]_5[OSi(OiPr)Me]$	1444.07160	1444.07162	0.0
$[O_{3/2}SiMe]_{14}[OSiMe_2]_4[OSi(OH)Me][OSi(OiPr)Me]$	1446.06334	1446.05105	8.5
$[O_{3/2}SiMe]_{18}[OSi(OiPr)Me]_2$	1460.00572	1459.99376	8.2
$[O_{3/2}SiMe]_{18}[OSiMe_2]_4$	1519.96915	1519.97895	−6.4
$[O_{3/2}SiMe]_{18}[OSiMe_2]_5$	1593.99762	1593.99772	−0.1
$[O_{3/2}SiMe]_{18}[OSiMe_2]_4[OSi(OiPr)Me]$	1638.03096	1638.02396	4.3
$[O_{3/2}SiMe]_{20}[OSiMe_2]_4$	1653.96610	1653.96445	1.0
$[O_{3/2}SiMe]_{18}[OSiMe_2]_6$	1668.01965	1668.01649	1.9
$[O_{3/2}SiMe]_{20}[OSiMe_2]_3[OSi(OiPr)Me]$	1697.99066	1697.99069	0.0
$[O_{3/2}SiMe]_{18}[OSiMe_2]_5[OSi(OiPr)Me]$	1712.04618	1712.04273	2.0
$[O_{3/2}SiMe]_{22}[OSiMe_2]_3$	1713.93441	1713.93122	1.9
$[O_{3/2}SiMe]_{20}[OSiMe_2]_5$	1727.98368	1727.98322	0.3

Note that these isomeric species cannot be distinguished by ESI-FTICR mass spectrometry since they have identical exact mass values and the neutral resin species are not subjected to chromatographic separation techniques prior to introduction into the mass spectrometer.

The average compositions for the methyl silsesquioxane resin for fractions 1 and 4 were found to be very similar. These were calculated from the structural assignments made from the ESI-FTICR data reported in Tables 1 and 2. The average structure for fraction 1 was found to be $[O_{3/2}SiMe]_{0.772}[OSiMe_2]_{0.172}[OSi(OH)Me]_{0.021}[OSi(OiPr)Me]_{0.035}$ while fraction 4 had an average structure of $[O_{3/2}SiMe]_{0.788}[OSiMe_2]_{0.174}[OSi(OH)Me]_{0.006}[OSi(OiPr)Me]_{0.032}$.

MALDI-TOFMS

Figures 5 and 6 show the mass spectra for the fractions 4, 8, 13, 18, 20, and 21. For the two low mass fractions individual oligomers can easily be identified in the spectra, as seen in Fig. 5. In the four higher mass fractions this resolution is lost. This occurs for two reasons: (i) time-of-flight mass separa-

Structure A

Structure B

T_4D_3

$T_4D_2T^{(OiPr)}$

Structure C

Structure D

T_6D_2

$T_6DT^{(OR)}$ R=H, iPr

Structure E

Structure F

Structure G

$T_4D_2T^{(OH)} T^{(OMe)}$

T_8D

T_6D_3

Structure H

Structure I

Structure J

$T_6D_2T^{(OR)}$ R=H, iPr

$T_6DT^{(OH)} T^{(OMe)}$

$T_8T^{(OiPr)}$

Structure K

Structure L

Structure M

T_{10}

T_8D_2

$T_8DT^{(OR)}$ R=H, iPr

Structure N

Structure O

$T_{10}D$

T_8D_3
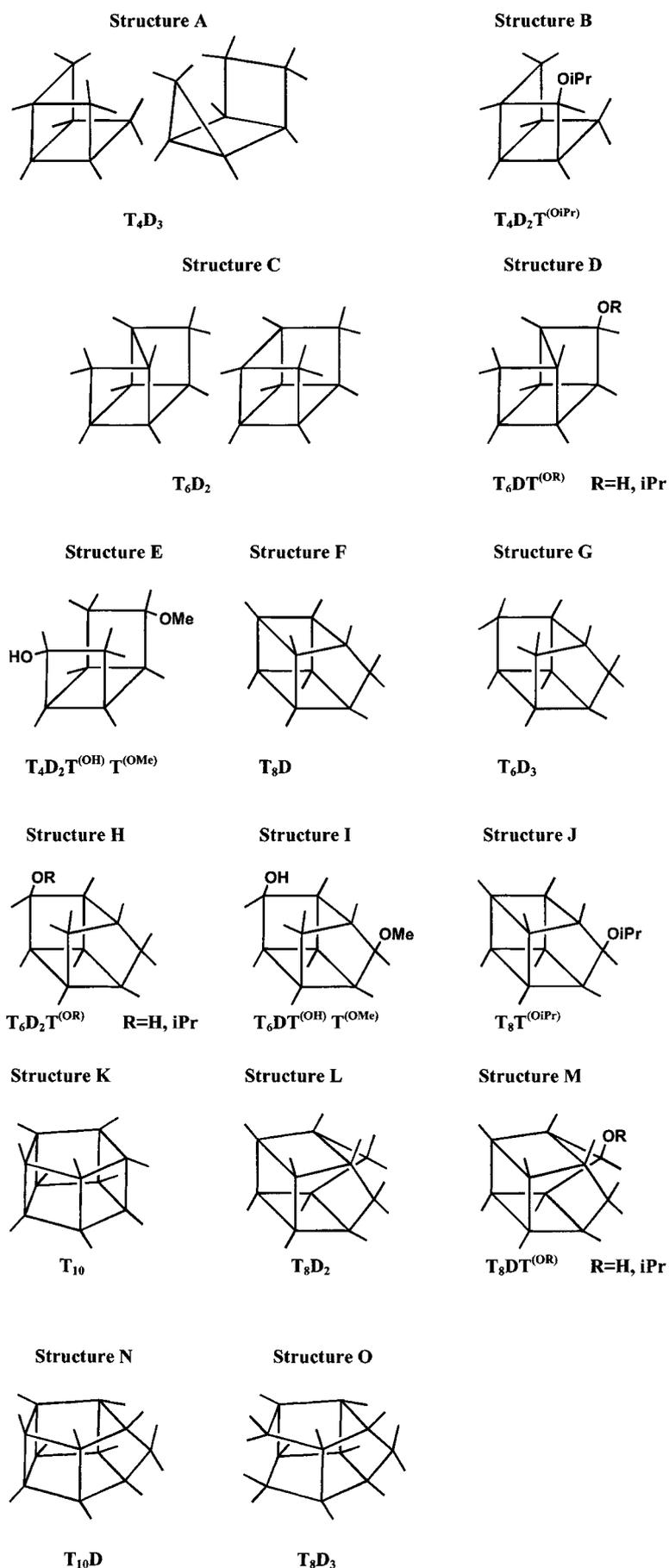
Figure 4. Individual methyl silsesquioxane structures from the ESI-FTICR data for fraction 1.

RCM
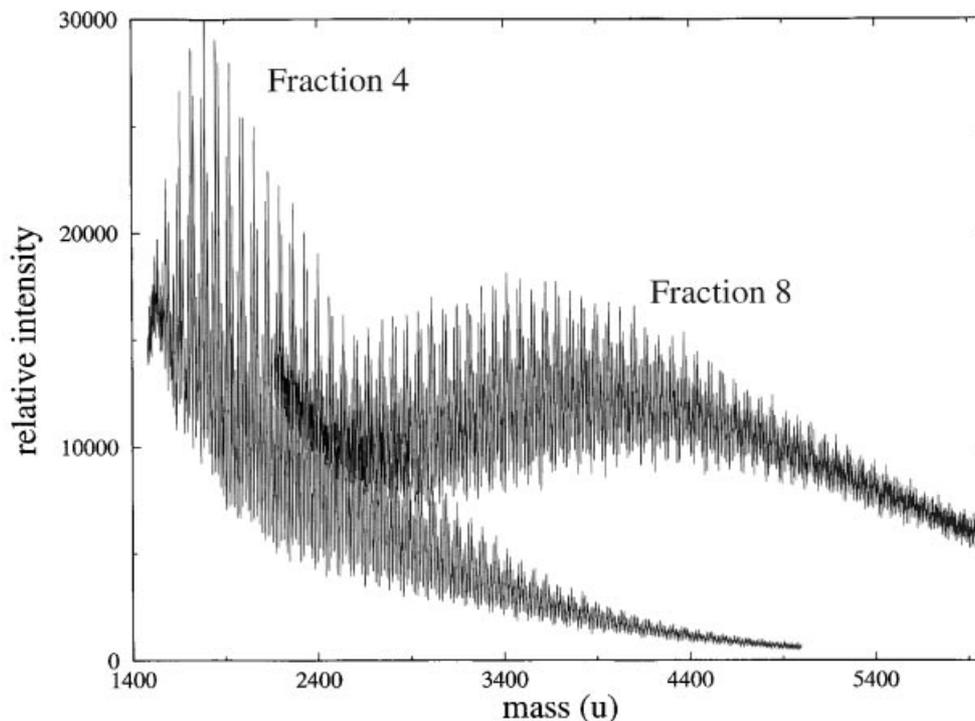
Figure 5. MALDI-TOF mass spectra of fractions 4 and 8.

tion loses resolution at higher mass by its very nature (time is proportional to the square root of mass); and (ii) since the analyte is a copolymer, the combinations of possible monomers lead to the 'peak at every mass' problem.

The molecular mass distributions were calculated for the five higher mass fractions and are given in Table 3 in comparison to the gel-permeation chromatography (GPC) analysis. (Due to the sweeping baseline, due mainly to matrix ions, a reliable molecular mass for fraction 4 could not be calculated.) The values of M_n from mass spectrometry are consistently higher with this difference steadily increasing with molecular mass. This is not surprising since GPC
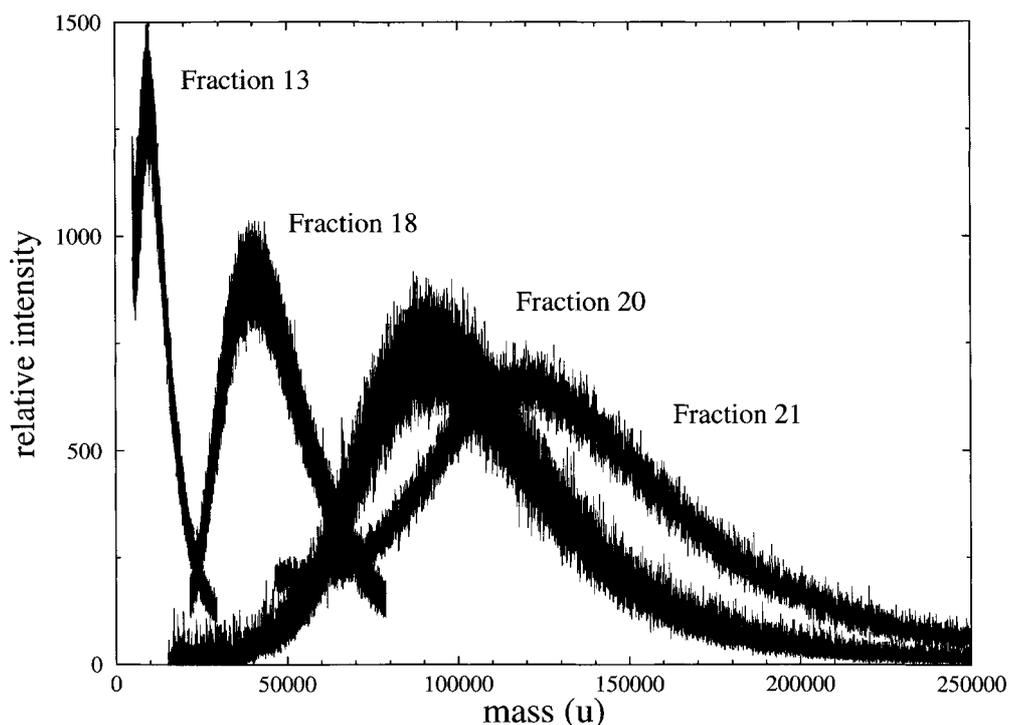
Figure 6. MALDI-TOF mass spectra of fractions 13,18, 20, and 21.

Table 3. Molecular mass distributions computed from MALDI-TOF mass spectra compared to gel-permeation chromatography values

Fraction	GPC M_n	Mass spec. M_n	Mass spec. M_w
8	3415 g/mol	3565 g/mol	3778 g/mol
13	9070	12,087	13,363
18	24,130	45,434	48,040
20	43,770	100,995	110,725
21	56,160	124,847	132,059

measures relative hydrodynamic radius and, as with close-packed structures as found in silsesquioxane resins, tends to underestimate the molecular mass from its determination of molecular radius in solution.[10,11] Thus, the MALDI-TOFMS values can be used to create a calibration curve for the GPC values.

DISCUSSION

The first observation is that few of the detected resin structures in Tables 1 and 2 contain residual unreacted silanol groups, and that no single structure contains more than one hydroxyl group. This suggests that compact cage structures arise from the efficient assembly of small siloxane rings. Furthermore, it is thought that the rapid condensation of silanol groups on adjacent and non-adjacent silicon atoms occurs and is catalyzed by the excess hydrochloric acid, formed during the initial hydrolysis step. With the exception of a weak signal for the $[O_{3/2}SiMe]_{10}$ molecule (structure **K**), no other species were observed with completely closed cages

containing only the $[O_{3/2}SiMe]$ group (see Tables 1 and 2). All other structures had lower symmetry and contained one or more of the following siloxy groups: $[OSiMe_2]$, $[OSi(OH)Me]$, $[OSi(OMe)Me]$, and $[OSi(OiPr)Me]$. Another observation drawn from analysis of the raw ESI-FTICR mass spectrum is that the most abundant resin species contained predominately odd numbers of silicon atoms. For example, numerous siloxane structures containing nine silicon atoms are observed in the ESI-FTICRMS data for fraction 1 (see structures **F, G, H, I** and **J**). This is commonly observed for silicone resin systems that are synthesized in polar hydrogen-bonding solvents. By contrast, silicone resins synthesized from chlorosilanes in non-polar aprotic solvents typically consist of highly symmetric closed cage structures with predominately even numbers of silicon atoms per molecule. Following hydrolysis of the chlorosilane reactants to hydroxysilanes, there are three types of chemical pathways that are thought to be operative in the synthesis of silsesquioxane resins: (i) intramolecular condensation; (ii) intermolecular condensation, and (iii) acid-catalyzed siloxane bond cleavage followed by insertion of small molecules containing silanol groups. Intramolecular silanol condensation may occur for siloxane rings containing five or more silicon atoms.

For the low mass fractions 1 and 4 the ESI-FTICR spectra have the necessary accuracy and precision for an exact mass analysis of the oligomers present. On the other hand, MALDI-TOFMS is not sufficiently precise for this type of analysis. Instead mass autocorrelation techniques[12] are used to look for general trends in the data rather than to attempt to identify each of the more than 100 discrete peaks in the spectra for fractions 4 and 8. The methods
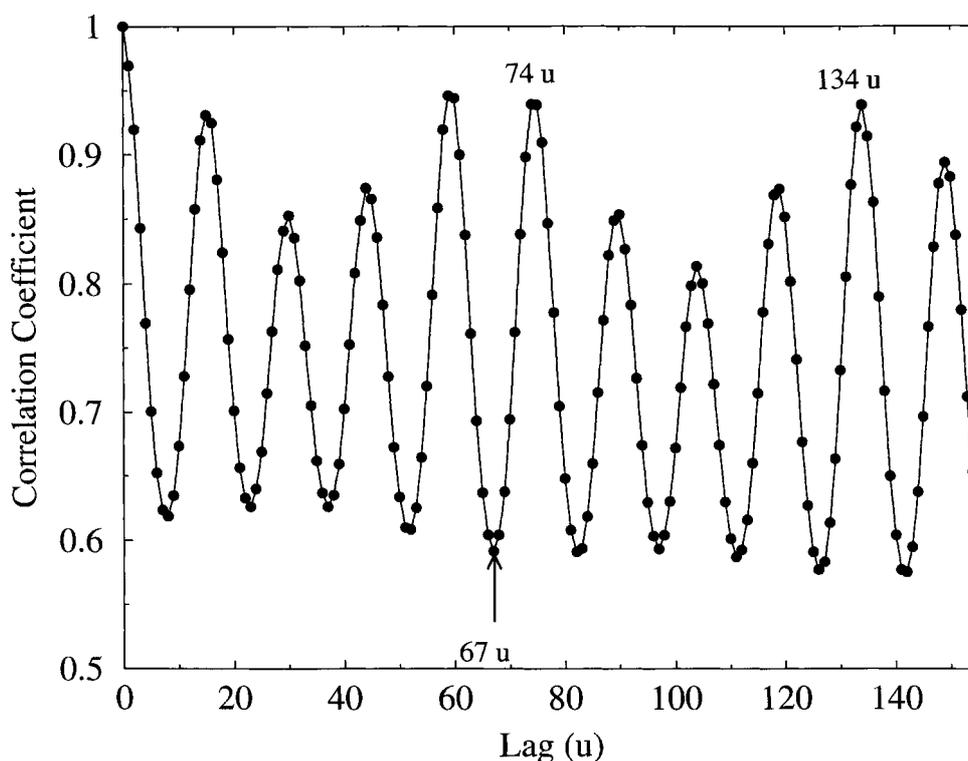
Figure 7. Mass autocorrelation of fraction 4.

used are well known in the area of discrete time-series analysis.

The mass autocorrelation function is defined as:

$$G(L) = \sum_i S(m_i)S(m_{i+L}) / \sum_i S(m_i)S(m_i) \qquad (1)$$

where $S(m_i)$ is the signal intensity at m_i where m_i takes integer values of mass and L is the mass lag which was allowed to range from (0 to 1000) u. The equation merely takes the product of two signal intensities separated by L mass units and normalizes this by the square of the signal intensity at the first point. To obtain the correct mass autocorrelation function, the original signal, which has data points that are periodic in time, was interpolated using a linear fit with periodic points in mass. This is because the mass spectrum presented in 'mass-space' does not have evenly spaced points in mass since the transform from time to mass is not linear but quadratic. Since the density of points varies across the mass spectrum in relation to the peak widths there is a necessary decrease in point density upon interpolation. To overcome this, points at integer values of mass (1 u, 2 u, 3 u, etc.) were used. These are more widely spaced than the original time-space points. This results in a decrease in the data-set length. This also resulted in the loss of isotopic resolution in the mass autocorrelation function but did enhance its 'smoothing' effect on the data.

Figure 7 shows the mass autocorrelation of fraction 4. Peaks appear in the mass autocorrelation at each of the repeat distances of the main spectrum. There is a large peak at 74 u indicative of the dimethylsiloxane [$OSiMe_2$] unit (D). That indicates that there frequently occur pairs of oligomers separated in mass by 74 u, i.e. that the higher mass oligomer

Table 4. Identification of peaks in the mass autocorrelation of the MALDI-TOF data using the relation |n2T - mD|

	n=	0	1	2	3	4
m=	0	0 u	134 u	268 u	402 u	536 u
	1	74 u	60 u	194 u	328 u	463 u
	2	148 u	14 u	120 u	254 u	389 u
	3	222 u	88 u	46 u	180 u	315 u
	4	296 u	162 u	28 u	106 u	240 u

has grown by one D unit. More importantly, there is no peak at 67 u, which is the mass of the methyl silsesquioxane [$O_{3/2}SiMe$] unit (T). However, there is a peak at 134 u, which is twice the mass of the silsesquioxane unit (2T). This immediately indicates that each oligomer present has an even number of T units. (This is confirmed by the observation that there are also peaks at 4T, 6T, 8T, etc., but not at 3T, 5T, 7T, etc.) This information, in combination with the observation from fractions 1 and 4 from the ESI-FTICR data that oligomers with an odd number of silicon atoms are more stable, may lead to a greater understanding of the topology of the higher mass oligomers. Each of the other peaks in the mass autocorrelation can be shown to be linear differences of 2T and D units forming the general function n2T-mD. Table 4 shows some of these combinations at lower mass. Notice that for every combination there is a peak in the mass autocorrelation and there are no peaks in the mass autocorrelation that are not in Table 4. Since the interpolation was done at 1 u intervals, there are uncertainties of 1 to 2 u between the table and the figure. The peak heights in Fig. 7 should be indicative of the combinatorial mathematics of
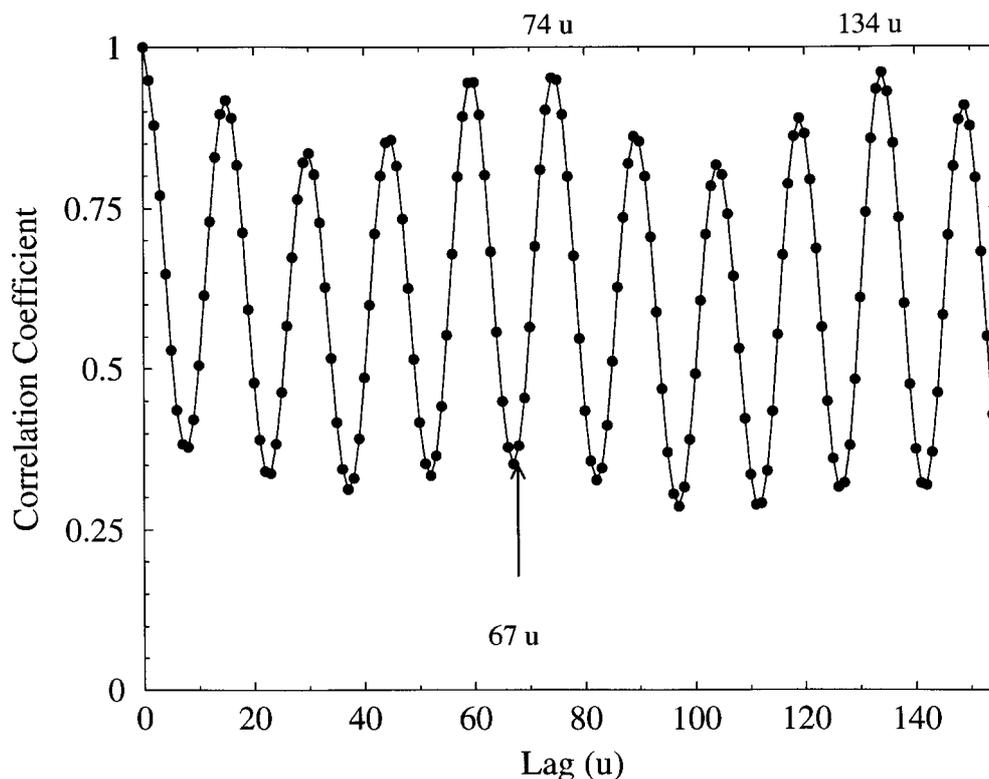
Figure 8. Mass autocorrelation of fraction 8.

combining D and 2T units in either a random or an ordered sequence. This hypothesis has yet to be substantiated experimentally.

The next observation to be made is that there is no peak at 18 u in the mass autocorrelation. The hydrolysis-condensation reaction used gives off water when two silanols combine to form a bridging oxygen. In incompletely condensed silsesquioxanes a strong mass autocorrelation peak is seen at 18 u indicative of oligomers with the same number of repeat units but different degrees of condensation.[13,14] The lack of a peak at 18 u immediately indicates that either full intramolecular condensation of silanols has taken place, or no intramolecular condensation of silanols has taken place. Only an exact indexing of peaks in the mass spectrum can answer this question; however, it seems unlikely that condensation can occur to polymerize the material (intermolecular condensation) with some concomitant intramolecular condensation also occurring. Additionally, an even number of T units is a strong indication of complete condensation since an odd number of T units would always leave at least one silanol in the material leading to further condensation reactions.

Figure 8 shows the mass autocorrelation for fraction 8. One observes that the two functions in Figs 7 and 8 have very similar relative peak intensities at the same peak positions. This is strong evidence that the topology of the higher fraction matches that of the lower fraction. This, in turn, indicates that the polymerization is a local, and not an extended chain, function. That is, larger oligomers are built up by the coalescence of smaller oligomers rather than by the addition of monomers in contrast to the ESI-FTICR exact mass analysis that suggested that the smallest oligomers are made by monomer addition to form stable ring structures. The greater difference in correlation coefficients between correlated and uncorrelated masses in Fig. 8 and compared to Fig. 7 derives from the fact that the fraction 4 data lies on a flatter background than the fraction 8 data (see Fig. 5).

CONCLUSIONS

A methyl silsesquioxane resin was carefully analyzed by a combination of ESI-FTICR and MALDI-TOFMS in order to determine its molecular structure. The exact mass analysis by ESI-FTICR was able to specifically identify low mass oligomers and was able to determine that closed structures predominated. The MALDI-TOFMS measurements determined that the molecular masses were twice as high as measured by GPC. Mass autocorrelation revealed that in this nearly fully condensed resin the silsesquioxane monomer occurs in even multiples.

REFERENCES

1. Brevett CS, Cagle PC, Klemperer WG, Ruben GC. *J. Inorg. Organometal. Polym.* 1991; **1**: 335.
2. Baney RH, Itoh M, Sakakibara A, Suzuki T. *Chem. Rev.* 1995; **95**: 1409.
3. Auner N, Bats JW, Katsoulis DE, Suto M, Tecklenburg RE, Zank GA. *Chem. Mater.* 2000; **12**: 3402.
4. Eisenberg P, Erra-Balsells R, Ishikawa Y, Lucas JC, Mauri AN, Nonami H, Riccardi CC, Williams RJJ. *Macromolecules* 2000; **33**: 1940.
5. Bakhtiar R, Feher FJ. *Rapid Commun. Mass Spectrom.* 1999; **13**: 687.
6. Maziarz EP, Baker GA, Wood TD. *Macromolecules* 1999; **32**: 4411.
7. McEwen CN, Jackson C, Larsen BS. *Int. J. Mass Spectrom. Ion Processes* 1997; **160**: 387.
8. Hensel RR, King RC, Owens KG. *Rapid Commun. Mass Spec.* 1997; **11**: 1785.
9. Frevel LK, Lee W, Tecklenburg RE. *J. Am. Soc. Mass Spectrom.* 1999; **10**: 231.
10. Grubisic Z, Rempp P, Benoit H. *J. Polym. Sci. B.* 1967; **5**: 753.
11. Guttman CM, DiMarzio EA. *Macromolecules* 1970; **3**: 681.
12. Wallace WE, Guttman CM. *J. Res. Natl. Inst. Stand. Technol.* 2001; *in press*.
13. Wallace WE, Guttman CM, Antonucci JM. *J. Am. Soc. Mass Spectrom.* 1999; **10**: 224.
14. Wallace WE, Guttman CM, Antonucci JM. *Polymer* 2000; **41**: 2219.